

Activated Metallic Gold as an Agent for Direct Methoxycarbonylation

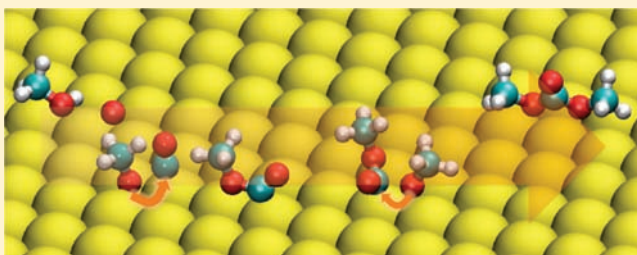
Bingjun Xu,[†] Robert J. Madix,[‡] and Cynthia M. Friend^{*,†,‡}

[†]Department of Chemistry and Chemical Biology, Harvard University, 12 Oxford Street, Cambridge, Massachusetts 02138, United States

[‡]School of Engineering and Applied Sciences, Harvard University, Cambridge, Massachusetts 02138, United States

 Supporting Information

ABSTRACT: We have discovered that metallic gold is a highly effective vehicle for the low-temperature vapor-phase carbonylation of methanol by insertion of CO into the O–H bond to form methoxycarbonyl. This reaction contrasts sharply to the carbonylation pathway well known for homogeneously catalyzed carbonylation reactions, such as the synthesis of acetic acid. The methoxycarbonyl intermediate can be further employed in a variety of methoxycarbonylation reactions, without the use or production of toxic chemicals. More generally we observe facile, selective methoxycarbonylation of alkyl and aryl alcohols and secondary amines on metallic gold well below room temperature. A specific example is the synthesis of dimethyl carbonate, which has extensive use in organic synthesis. This work establishes a unique framework for using oxygen-activated metallic gold as a catalyst for energy-efficient, environmentally benign production of key synthetic chemical agents.



INTRODUCTION

Concern for environmental toxicity and high energy consumption in large-scale chemical syntheses has driven recent efforts to develop processes that minimize adverse environmental impact. Catalysis has a central role in green chemistry because of its potential to lower the operation temperatures in reactors and to increase the selectivity for specific, desirable products. Heterogeneous catalysts are particularly desirable because they exist in a phase separate from the reactants and products and, thus, are completely recoverable, do not require energy-consuming separation processes, and do not themselves contribute to toxic byproducts.

Rh-, Co-, and Ir-based homogeneous catalysts are well-known for their versatility for a wide variety of carbonylation reactions.¹ In the case of the methanol carbonylation to form acetic acid, CO is inserted into a methyl–Rh bond, methanol having been activated by HI in solution. Subsequent hydrolysis of the coordinated acetyl (with the aid of iodide) produces acetic acid. Similarly, carbonylation of alkenes (hydroformylation) involves insertion of CO into an Rh–alkyl bond and reductive elimination of the aldehyde product.

More recently, supported Au catalysts promoted by halides were used to try to mimic the homogeneous carbonylation of methanol to acetic acid in the vapor phase^{2,3} using gaseous mixtures of methanol, hydrogen, methyl iodide, and CO at high pressure (250 psi). Methyl acetate, not acetic acid, is the dominant product with no dimethyl carbonate reported. Although the exact mechanistic steps are still unclear, the use of the halide promoter is critical, suggestive of pathways similar to the homogeneous processes.

Herein we report the discovery of a direct, CO addition reaction facilitated by metallic gold for the synthesis of methoxy-

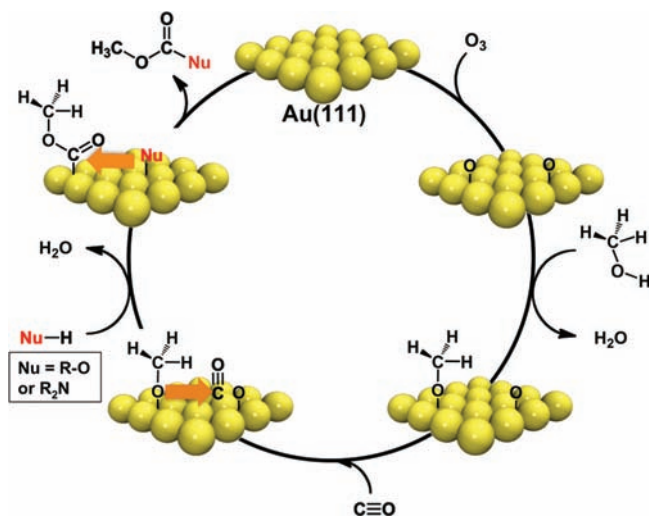
carbonyl, which has the potential for methoxycarbonylation of alcohols and amines,⁴ transesterification of glycerol to glycerol carbonate,⁵ as well as selective production of other related carbonate products, e.g., dialkyl carbonates and alkyl carbamates.⁶ No halide promoter is necessary, and the reaction steps are distinct from those governing the classical carbonylation of methanol. There is precedence for formation of methoxycarbonyl by homogeneous Pd(II) phosphine complexes, identified using IR and NMR albeit at very high CO pressures (20–144 atm).⁷ Even so, the products of these solution-phase reactions are dimethyl oxalate and acetic acid for both homogeneous Pd complexes and supported heterogeneous Pd.⁸

The basic principles governing the reactions of the methoxycarbonyl species on Au activated by oxygen are clearly illustrated and explained. Primary emphasis is given here to the oxygen-assisted catalytic carbonylation of methanol to synthesize dimethyl carbonate (Scheme 1, Nu = CH₃O, RO, or R₂N), a key “green” synthetic reagent, with mild reaction conditions without the production of toxic byproducts. The overall principle of the reactions is generalized by reactions with dimethylamine and other alcohols, distinguishing this work from prior studies.

The potential impact of a green, heterogeneous process for methoxycarbonylation is broad. For example, dimethyl carbonate is used for major applications, including a fuel additive,⁹ a solvent,¹⁰ and a reagent in transesterification reactions critical to biodiesel production;¹¹ it is used for methylation and methoxycarbonylation processes in organic synthesis.⁶

Received: August 23, 2011

Published: October 28, 2011

Scheme 1. Gold-Mediated Carbonylation^a

^a Carbonylation of the surface-bound methoxy gives adsorbed methoxycarbonyl to which a surface nucleophile (Nu in the graphic, e.g., alkoxy or amide) adds to form the corresponding coupling product.

Moreover, large-scale production of dimethyl carbonate on an industrial scale is anticipated to increase in order to meet current and future demands: 170 tons/day were produced in 1997. China recently added a capacity of 267 000 ton/year,¹² and the estimated future demand (300 000–600 000 ton/year) is 5–10 times that of the current U.S. production capacity.¹³ Clearly, efficient catalytic production of dimethyl carbonate and/or an alternate route for methoxycarbonylation would have a major impact. Though it is a substitute for highly toxic reagents, such as methyl halides and phosgene (COCl_2), which were traditionally used as methylation reagents and produce halides as harmful byproducts,⁶ its production is *not* without environmental impact, typically requiring high pressures and/or temperatures and yielding HCl as a byproduct.⁹

Only oxygen, CO, and methanol are used in the direct carbonylation of methanol on gold reported here. The potential advantages of the oxygen-assisted gold-catalyzed synthesis are that (1) it proceeds at low temperatures for a wide range of selective bond scission processes,^{14–21} (2) is tolerant to the presence of water, and (3) is potentially very selective. We show here that gold is, in fact, extremely active for production of dimethyl carbonate as well as other coupled organic carbonates when activated by atomic oxygen.

EXPERIMENTAL DETAILS

Experimental Setup, Surface Cleaning, and Reactant Dosing. Experiments were performed in two separate ultrahigh vacuum (UHV) chambers. Temperature programmed reaction (TPR) and high-resolution electron loss spectroscopy (HREELS) experiments were conducted in a UHV chamber with a base pressure below 2×10^{-10} Torr. The single crystal Au(111) surface was cleaned by repeated Ar sputtering and annealing cycles, as confirmed by Auger electron spectroscopy (AES) and low energy electron diffraction (LEED) measurements.²² The surface was first populated with 0.1 ML O ($\text{O}/\text{Au}(111)$) by dosing an appropriate amount of ozone at 200 K. The oxygen atom coverage was calibrated by comparing the amount of O_2 evolution at ~ 550 K in temperature programmed desorption to that

evolved from a surface saturated with oxygen atoms, which is 1.1 ML.²³ The oxygen coverage reported is an average value, and the local oxygen coverage can deviate significantly from the mean value. The error in oxygen coverage on the Au(111) surface is $\pm 15\%$ due to day-to-day variation in O_3 concentration. Oxidation of the surface in this manner leads to release of Au atoms to form nanostructures containing Au and O, most of which are smaller than 2 nm in diameter.²² Oxygen is primarily bound in local 3-fold coordination sites using this preparation.

Methanol and CO were sequentially introduced onto the oxygen-covered surface at 150 K via leak valves. Exposures, corrected for dosing enhancement, are given here in terms of Langmuir (L, 1 Langmuir = 1×10^{-6} Torr seconds). The total pressure rise in the vacuum chamber during the dosing of the reactants was used as a measure of the total exposure. Unless otherwise noted, 6 L was the typical dose.

Temperature Programmed Reaction Spectroscopy. Temperature programmed reaction experiments were used to determine product distributions and were performed according to well-established protocol.²² In a typical experiment, Au(111) with reactants adsorbed was heated up linearly (~ 5 K/s) in front of a quadrupole mass spectrometer (Hiden HAL/3F). The selectivity for formation of different products is derived from experimental measurements analyzed using the following equation

$$S_i = \frac{n_i}{\sum_i n_i}$$

in which S_i is the selectivity toward product i and n_i is the number density of the product i detected in the mass spectrometer. In the present case, the only products observed are dimethyl carbonate, methyl formate, CO_2 , and water. No formaldehyde and formic acid were formed at a detectable level. The number density of product i is obtained using the integrated area under the signature mass peaks (90, 60, and 44 amu for dimethyl carbonate, methyl formate and CO_2 , respectively), corrected for fragmentation, ionization cross-section, transmission coefficient, and detection efficiency.²⁴

Vibrational and X-ray Photoelectron Spectroscopy. Vibrational spectra (Figure 4a) were obtained using high resolution electron energy loss spectroscopy collected with an LK2000 spectrometer using a primary energy of 7.17 eV at 60° specular geometry. All spectra were taken at 150 K with a full width of half max $70\text{--}80\text{ cm}^{-1}$. The X-ray photoelectron spectroscopy (XPS) experiments were conducted in a second chamber, with a base pressure below 5×10^{-10} Torr. X-ray photoelectron spectra were acquired with an analyzer passing energy of 17.9 eV and a multiplier voltage of 3 kV using Mg $K\alpha$ X-rays (300 W) as the excitation source. The binding energy (BE) calibration was referenced to the Au $4f_{7/2}$ peak at 83.9 eV. The O(1s) spectra were accumulated with 100 scans to enhance the signal-to-noise ratio.

The spectra in Figure 4b were used to deconvolute the functional O(1s) binding energies due to different species on the surface. First, the peak position and width characteristic of atomic oxygen were obtained by using a single Gaussian peak to fit the trace in Figure 4b-i. Subsequently, the spectrum in 4b-ii was used to obtain peak parameters for methoxy bound to gold by fitting with 2 Gaussian peaks, one of which uses the same parameters as for adsorbed oxygen (Figure 4b-i); the other peak is attributed to methoxy. Finally, the trace in Figure 4b-iii was fit with three Gaussians, two of which use the parameters for atomic oxygen and methoxy. The third peak was decomposed into two oxygen peaks, attributed to the inequivalent oxygens in methoxycarbonyl. These peaks were assigned by comparison to model compounds that contain the same functional groups, dimethyl carbonate and methyl formate (Figure S4 and Table S4). The width and area of the peaks attributed to oxygen in the methoxy group and the carbonyl group of methoxycarbonyl were set to be identical in this final fitting process.

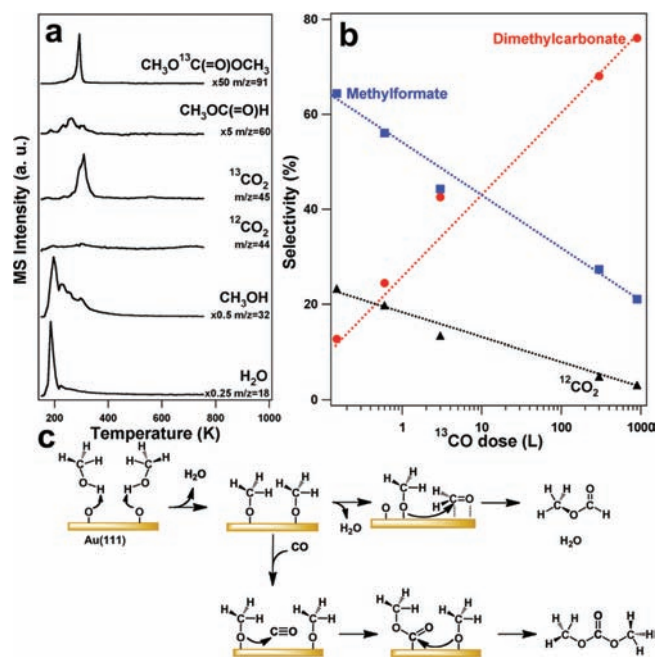


Figure 1. (a) Temperature programmed reaction showing dimethyl carbonate ($\text{CH}_3\text{O}^{13}\text{C}(=\text{O})\text{OCH}_3$), methyl formate ($\text{CH}_3\text{OC}(=\text{O})\text{H}$), $^{13}\text{CO}_2$, and water formed in the reaction of methanol with ^{13}CO on Au(111) activated by 0.1 monolayer (ML) of O. (b) The change in product selectivity for coupling products and $^{12}\text{CO}_2$ (from combustion of methanol) on the amount of ^{13}CO dosed onto the methoxy-covered surface. (c) Pathways for the competing coupling pathways: oxidative self-coupling of methanol to methyl formate (upper) and coupling to CO yielding dimethyl carbonate (lower). The reactant dose used in part a corresponded to an integrated flux of 6 Langmuirs (L) (the equivalent of 6 layers) of methanol and 900 L of ^{13}CO . Six L of methanol is used in all experiments in part b.

RESULTS AND DISCUSSION

The direct carbonylation of methanol on metallic gold proceeds via nucleophilic attack on the carbon atom in CO by methoxy bound to the gold surface to yield the surface intermediate methoxycarbonyl (Figure 1 and Scheme 1). In order to form dimethyl carbonate a second surface-bound methoxy then adds to this species. The methoxy is formed from selective activation of methanol by adsorbed atomic oxygen. The only byproducts of this reaction are water, CO_2 , and methyl formate. In order to establish this mechanism methanol and ^{13}CO were sequentially introduced to a Au(111) surface with 0.1 monolayer of adsorbed atomic oxygen (O/Au(111)) at 150 K (Figure 1). The oxygen was deposited using ozone decomposition under conditions that produce O-covered Au nanoparticles, most of which are ~ 2 nm in diameter.²² Importantly, the oxygen is required for reaction. Methanol desorbs without reaction from either flat Au(111) or from Au(111) containing the Au nanoparticles from which the oxygen is first removed.²⁵ The carbonylation product, $\text{CH}_3\text{O}^{13}\text{C}(=\text{O})\text{OCH}_3$, was produced upon heating (295 K) along with the self-coupling product, $\text{CH}_3\text{OC}(=\text{O})\text{H}$ (methyl formate) (230 K). The activation energy of the carbonylation reaction is estimated to be ~ 75 kJ/mol, assuming a pre-exponential factor of 10^{13} s^{-1} . Unreacted methanol and secondary oxidation products also evolved from the surface (Figure 1a).

The use of ^{13}CO and $^{12}\text{CH}_3\text{OH}$ firmly establishes that two methoxy species react with a single ^{13}CO . The only products

other than $\text{CH}_3\text{O}^{13}\text{C}(=\text{O})\text{OCH}_3$ that formed are unlabeled methyl formate, $^{13}\text{CO}_2$, $^{12}\text{CO}_2$, and H_2O . The small yield of $^{12}\text{CO}_2$ at the highest dose of ^{13}CO shows that the majority of combustion under the conditions of Figure 1a is due to oxidation of ^{13}CO , not methanol. Parallel studies of ^{12}CO with methanol on O/Au(111) verified that a single CO is incorporated into the product, on the basis of the mass shift of the product parent ion by one unit. Product identification was authenticated by quantitative comparison of the fragmentation patterns of the products and the corresponding neat samples or reference data from NIST (see Supporting Information, Figure S1 and Table S1).

The competing pathway of oxidative self-coupling of methanol to methyl formate (Figure 1c) was previously established from model studies on oxygen-covered Au(111)¹⁵ and under catalytic conditions on nanoporous gold.²⁶ The salient features of the mechanism are that atomic O on Au initiates the reaction by inducing O–H bond scission to yield methoxy bound to the surface. Methyl formate is formed after a fraction of the methoxy eliminates a methyl hydrogen to produce formaldehyde. Attack of the electron-deficient carbon in formaldehyde by the remaining methoxy leads to the coupling product.¹⁶ Importantly, elimination of hydrogen from adsorbed methoxy to produce formaldehyde is the rate-determining step for this reaction; thus, methoxy is sufficiently stable to be used as a reagent for the syntheses of the carbonate (Figure 1c).

The $\text{CH}_3\text{OC}=\text{O}(\text{ads})$ intermediate is stable at 150 K, suggesting that the carbonylation to form dimethyl carbonate is a two-step process (Figure 2a). The two-step nature of this methoxy addition was further verified by the introduction of CD_3OH after formation of a coadsorbed mixture of CH_3OCO and CH_3O , which adds adsorbed CD_3O to the surface via an acid–base surface displacement of CH_3O (Figures 2b and S2).²⁴ Subsequent heating initiates the nucleophilic attack of the methoxy carbonyl intermediate by $\text{CD}_3\text{O}(\text{ads})$ to produce $\text{CH}_3\text{OC}(=\text{O})\text{OCD}_3$, clear evidence for the final reaction of the methoxy-(D) with adsorbed methoxycarbonyl. Spectroscopic data, described below, confirm the identification of the methoxycarbonyl ($\text{CH}_3\text{OC}=\text{O}$) intermediate and provide insight into its structure.

This two-step addition of nucleophiles to CO has potential utility for a broad range of important, large-scale synthetic processes. Methoxycarbonylation can be accomplished catalytically on oxygen-activated metallic gold, possibly obviating the need for dimethyl carbonate in alkylcarbonylation reactions, such as carboxymethylation and transesterification for which it is used.⁴

Indeed, we have observed the formation of $\text{CH}_3\text{OC}(=\text{O})\text{OR}$, where R is ethyl or phenyl, and production of $\text{CH}_3\text{OC}(=\text{O})\text{N}(\text{CH}_3)_2$ from reaction with dimethyl amine via direct methoxycarbonyl transfer to the adsorbed dimethyl amide and phenoxy on metallic gold (Figure 3), demonstrating the generality of the reaction pathway reported here. Carbamates, formed by the surface-bound amide attacking the methoxycarbonyl intermediate, are widely used as herbicides, pesticides, drug intermediates, and precursors in the polymer industry.²⁷ The general two-step nucleophilic attack mechanism is shown in Scheme 2, in which the first surface nucleophile attacks CO at low temperature (150 K) forming a stable surface-bound intermediate, which is then attacked by a second nucleophile at higher temperature (~ 300 K) forming the final product. Although different nucleophiles react with the methoxycarbonyl intermediate, we have not yet observed direct carbonylation of ethoxy, phenoxy, or dimethyl

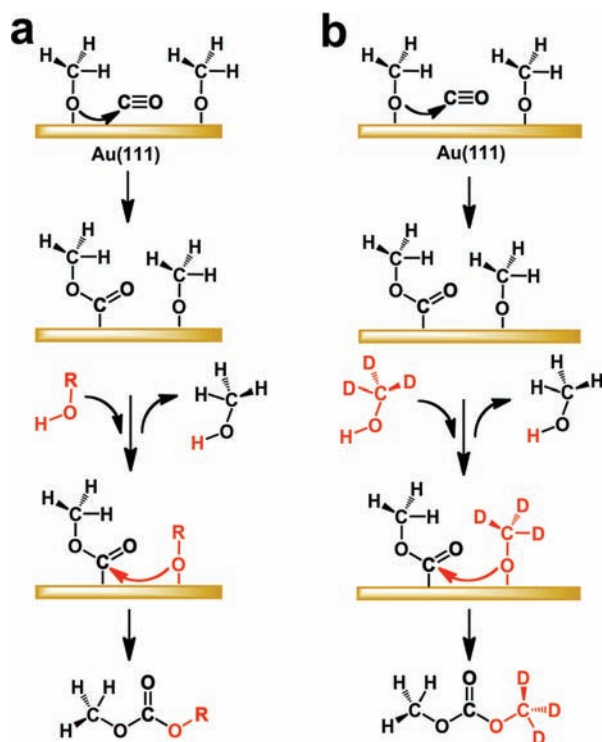


Figure 2. (a) Schematic of the carbonylation process via two successive nucleophilic attacks to form “asymmetric” carbonylated product. (b) Schematic from part a exemplified by $\text{CH}_3\text{O(a)}$ and $\text{CD}_3\text{O(a)}$. The second nucleophile ($\text{CD}_3\text{O(a)}$) was introduced to the surface via the partial surface displacement between CD_3OH and $\text{CH}_3\text{O(a)}$.

amide under the limited conditions tested. Further study is in progress to understand why this is the case. Nevertheless, the formation of methoxycarbonyl by CO addition to adsorbed methoxy provides a platform for a range of syntheses.

As expected from the mechanism shown in Scheme 1, the branching ratio for the two competing coupling pathways involving methanol and CO (methyl formate and dimethylcarbonate production) depends strongly on the amount of ^{13}CO introduced to the surface covered by adsorbed methoxy (Figure 1b). Exposure to a relatively small amount of ^{13}CO results in excess adsorbed methoxy, accounting for the dominance of methyl formate production and further combustion of methoxy by excess adsorbed oxygen.¹⁵ Conversely, increasing the amount of ^{13}CO dosed increases the selectivity for dimethyl carbonate formation because a larger fraction of the adsorbed methoxy is converted to the adsorbed methoxycarbonyl, leading to more dimethyl carbonate. Ultimately, the selectivity can be increased to 75% dimethyl carbonate, with methylformate accounting for about 23% and a negligible amount of $^{12}\text{CO}_2$ (Figure 1a). While the details have not been investigated for the other reactions of methoxycarbonyl with a second nucleophile, similar selectivity changes are expected (Figure 1a).

The formation of the adsorbed methoxycarbonyl intermediate was confirmed using vibrational and photoelectron spectroscopies. The vibrational bands characteristic of methoxy are observed after introduction of methanol to the oxygen-covered surface at 150 K¹⁵ (Figure 4a, middle trace). After the surface-bound methoxy is exposed to CO, new vibrational peaks appear that signify formation of $\text{CH}_3\text{OC}=\text{O(ads)}$ (Figure 4a, top trace). Comparison of the vibrational spectrum for dimethyl carbonate itself (Figure 4a,

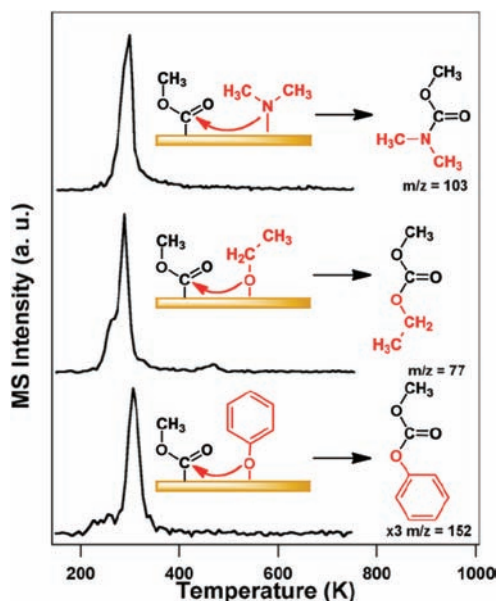
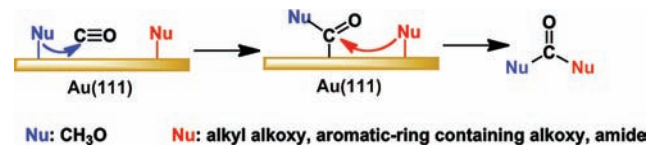


Figure 3. Carboxymethylation via direct methoxycarbonyl transfer to dimethyl amide (top), ethoxy (middle), and phenoxy (bottom). The intermediates shown were created by reaction of dimethylamine, ethanol, and phenol with 0.1 ML adsorbed O. Parent ions of the products are shown in each case.

Scheme 2. Generalized Two-Step Nucleophilic Attack Mechanism



bottom trace) with that of the intermediate (Figure 4a, middle trace) shows that dimethyl carbonate is *not* yet formed under these conditions. There is precedence for formation of methoxycarbonyl in Pd(II)–phosphine complexes and on Ni(111).^{7,28} (See Table S2, Supporting Information, for vibrational assignments.)

Density functional theory (DFT) calculations establish that methoxycarbonyl is a stable intermediate and provide the basis for vibrational assignments. On flat Au(111), the most favorable binding site of methoxycarbonyl is atop a single Au atom with the $\text{CH}_3\text{—O—C}=\text{O}$ plane perpendicular to the surface (Figure 5). (See Supporting Information for calculational details.) The band at 1655 cm^{-1} is assigned primarily to the $\text{C}=\text{O}$ double bond stretch on the basis of our calculations and analogous modes in organic esters (Table S2). The mode at 1040 cm^{-1} is ascribed to the asymmetric $\text{H}_3\text{C—O—C}$ stretch in the $\text{CH}_3\text{OC}=\text{O(ads)}$ (Table S2). Isotopic shifts further confirm these assignments. When ^{13}CO is used instead of ^{12}CO , the $\nu(\text{C}=\text{O})$ mode shifts from 1650 to 1620 cm^{-1} , which agrees well with the predicted isotopic red shift of 29 cm^{-1} (Figure 4a, inset). Thus, the C atom of the $\text{C}=\text{O}$ in the adsorbed methoxycarbonyl intermediate originates from CO (Figure 1c). There is also a small (10 cm^{-1}) downward shift for the $\nu(\text{C—O})$ mode, which is consistent with the ^{13}C substitution. The weak band at 2065 cm^{-1} is attributed to the $\text{C}=\text{O}$ stretch mode of a small amount of residual CO on the

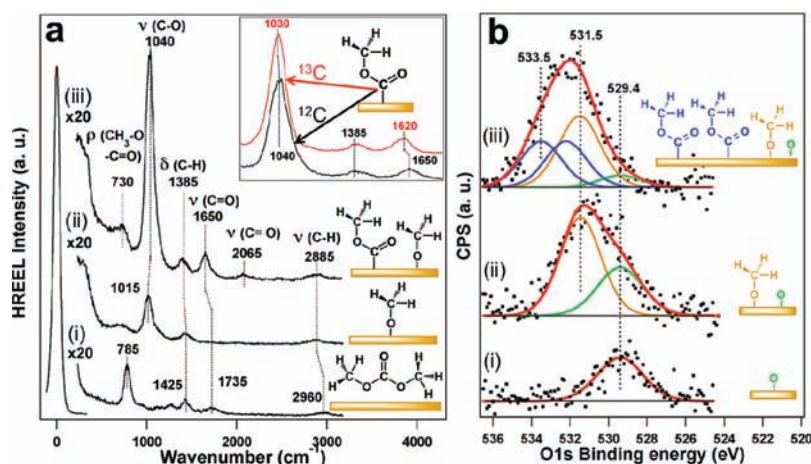


Figure 4. Formation of the surface intermediate $\text{CH}_3\text{OC}=\text{O}(\text{ads})$ is confirmed by both vibrational spectroscopy and X-ray photoelectron spectroscopy (XPS). (a) Electron energy loss spectra show the characteristic vibrations of (i) dimethylcarbonate, (ii) methoxy, and (iii) a mixture of methoxy and the surface intermediate, $\text{CH}_3\text{OC}=\text{O}$. The inset shows isotopic shifts in the spectra of $\text{CH}_3\text{O}^{12}\text{C}=\text{O}(\text{ads})$ and $\text{CH}_3\text{O}^{13}\text{C}=\text{O}(\text{ads})$. (b) The evolution of surface species reflected by O (1s) binding energies measured using X-ray photoelectron spectroscopy: (i) 0.1 monolayer of oxygen on Au(111), (ii) after introduction of (i) to methanol (6 L or the equivalent of 6 layers) showing the formation of methoxy (O 1s BE = 531.5 eV), and (iii) after introducing 300 L of CO to the surface to convert methoxy to the methoxy carbonyl intermediate [peaks in blue at 533.5 and 532.2 eV are assigned to the C=O and CH₃O moieties within methoxycarbonyl based on comparison with model compounds (Figure S4 and Table S4, Supporting Information)]. All experiments were performed at 150 K.

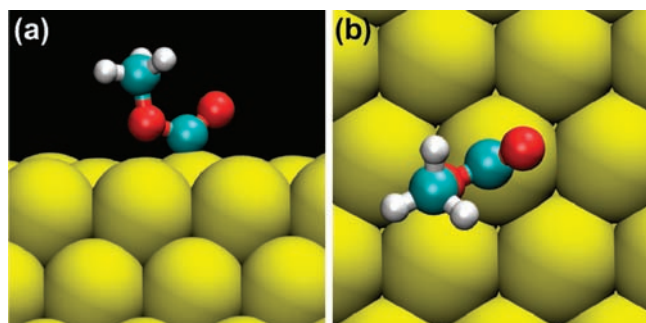


Figure 5. Calculated structure of methoxycarbonyl on Au(111): (a) side view and (b) top view. Large yellow spheres, red spheres, blue spheres, and small white spheres represent Au, O, C, and H atoms, respectively. Computational details are in Supporting Information.

surface.²⁹ A more detailed analysis of experimental and computed vibrational frequencies is in Supporting Information, Table S3 and Figure S3.

Since we know that gold nanoparticles form on our surface as a result of oxidation of Au(111),²² and since surface heterogeneities are present under most oxidative conditions (including catalytic conditions), DFT calculations were performed for a surface containing Au adatoms ($1/9$ monolayer) to evaluate whether defects alter the vibrational frequencies of this methoxycarbonyl species or its binding. The calculated vibrational frequencies shifted only slightly when methoxycarbonyl is adsorbed on an Au adatom, but the assignments remain the same. Binding of the $\text{CH}_3\text{O}-\text{C}=\text{O}$ to a Au adatom is more stable than on flat Au(111) by ~ 0.6 eV. To fully understand the role of defects, a thorough investigation of the activation energies for methoxycarbonyl formation on a variety of defects, including stepped surfaces, is required and is beyond the scope of this work.

Corresponding X-ray photoemission spectra provide further evidence for the $\text{CH}_3-\text{O}-\text{C}=\text{O}$ intermediate and quantify the

amount of conversion (Figure 4b). Upon introduction of methanol at 150 K, an O(1s) peak characteristic of methoxy appears at 531.5 eV³⁰ in addition to the peak for adsorbed atomic oxygen (529.4 eV).^{14,22} Introduction of 300 L of CO at 150 K gives rise to peaks at 532.2 and 533.5 eV of equal magnitude (shown in blue in Figure 4b-iii), consistent with the binding energies expected for adsorbed $\text{CH}_3-\text{O}-\text{C}=\text{O}$, based on model compounds (Figure S4, Table S4).

The potential relevance of our fundamental studies to working catalytic processes is suggested by our previous studies of methanol esterification over nanoporous gold.²⁶ Model studies on metallic Au(111) activated by atomic oxygen show methanol esterification to methyl formate with nearly 100% selectivity. The selectivity and activity of this model catalyst directly paralleled those of a nanoporous gold catalyst operated continuously at atmospheric pressure in flowing methanol and O₂. Similarly, there are strong parallels between our model studies of other coupling reactions on Au(111) and the product distributions of catalytic processes using either gold powder³¹ or Au supported on metal oxides in solution.^{18,26,32} The ability to relate the chemical activity of gold under controlled conditions at lower pressures and lower temperatures to its behavior under higher pressure conditions is most likely due to the fact that gold itself is not very active for bond breaking processes; thus, the steady state coverage of oxygen and other reaction intermediates on Au is rather low, even at higher pressures, a condition that can be mimicked at lower pressure and temperature. Similar correspondence has been observed for the selective oxidation of methanol to formaldehyde on silver catalysts.^{33,34} Hence, our model studies provide the understanding of the mechanisms of these reactions as guidelines for designing catalytic processes.

The oxygen-assisted methoxycarbonylation pathway described in this work is fundamentally different from the classic carbonylation of methanol to acetic acid on Rh-based catalysts. In solution methanol is activated by HI, the resultant CH₃I oxidatively adding to the Rh-complex. In our work methanol is activated

by atomic oxygen adsorbed on the gold surface to form adsorbed methoxy and water, and *no iodine-containing promoter is required*. Further, in the work reported here, CO inserts into the CH₃O–Au bond to form adsorbed methoxycarbonyl (CH₃OCO), whereas in the homogeneous process CO inserts into the CH₃–Rh bond to form acetyl. Lastly, in the gold-catalyzed methoxycarbonylation reported here a second nucleophile adds to the methoxycarbonyl to produce the products (e.g., carbonates, carbamates, Scheme 2), whereas reductive elimination of MeCOI with subsequent hydrolysis yields acetic acid in the Rh-catalyzed reaction. Though the mechanism of the carbonylation reaction on the supported gold catalyst is not yet known in detail, it appears strongly derivative of the homogeneous system. Iodide coordinated to Au is proposed to be an integral part of the active site for the carbonylation reaction,³⁵ and the products of the reaction are methyl acetate and acetic acid. Thus, the mechanism of carbonylation reported here differs fundamentally from that of previously reported work.

Metallic gold has the added advantage that it is recoverable and reusable. The mechanism established by our work provides a more direct route that could enhance the efficiency of these reactions and reduce the production of undesirable side products. Our work clearly establishes the need to determine the practical potential of gold for carbonylation processes through investigation under working catalytic conditions.

CONCLUSIONS

We demonstrate that the oxygen-activated Au surface efficiently mediates direct carbonylation of methoxy via a unique two-step nucleophilic attack mechanism. Methoxy nucleophilically attacks the carbon atom in CO to form a stable surface intermediate, methoxycarbonyl. Methoxycarbonyl is subsequently attacked by residual methoxy, leading to the formation of dimethyl carbonate, a green methylation agent. Other nucleophiles introduced to surface after methoxycarbonyl formation also react to yield, e.g., methyl ethyl carbonate (CH₃OC(=O)OC₂H₅) or CH₃OC(=O)N(CH₃)₂, demonstrating the generality of this pathway for methoxy carbonylation. The gold-mediated direct methoxycarbonylation has the potential for streamlining carboxymethylation and transesterification reactions, obviating the need for dimethyl carbonate.

ASSOCIATED CONTENT

S Supporting Information. Procedures for product identification using mass spectrometry, assignments of vibrational peaks, DFT calculational details, and XPS reference spectra and assignments. This material is available free of charge via the Internet at <http://pubs.acs.org/>.

AUTHOR INFORMATION

Corresponding Author
cfriend@seas.harvard.edu

ACKNOWLEDGMENT

We gratefully acknowledge the support of the U.S. Department of Energy, Basic Energy Sciences, under Grant DE-FG02-84-ER13289 (C.M.F.), and the National Science Foundation, Division of Chemistry, Analytical and Surface Science (R.J.M.) CHE-0952790. B.X. also acknowledges the Harvard University Center for the Environment for support through the Graduate Consortium in Energy and the Environment.

REFERENCES

- (1) Haynes, A. Acetic Acid Synthesis by Catalytic Carbonylation of Methanol. Jacobi von Wangelin, A.; Neumann, H.; Beller, M. Carbonylations of Aldehydes. In *Catalytic Carbonylation Reactions*; Beller, M., Ed.; Springer-Verlag: Berlin, 2006; Vol. 18, pp 179–221.
- (2) Zoeller, J. R.; Singleton, A. H.; Tustin, G. C.; Carver, D. L. U.S. Patent US6509293B1, Eastman Chemical Company, 2003.
- (3) Zoeller, J. R.; Singleton, A. H.; Tustin, G. C.; Carver, D. L. U.S. Patent US6177380B1, Eastman Chemical Company, 2001.
- (4) Ono, Y. *Catal. Today* **1997**, *35*, 15.
- (5) Ochoa-Gómez, J. R.; Gómez-Jiménez-Aberasturi, O.; Maestro-Madurga, B.; Pesquera-Rodríguez, A.; Ramírez-López, C.; Lorenzo-Ibarreta, L.; Torrecilla-Soria, J.; Villarán-Velasco, M. C. *Appl. Catal., A* **2009**, *366*, 315.
- (6) Tundo, P.; Selva, M. *Acc. Chem. Res.* **2002**, *35*, 706.
- (7) Rivetti, F.; Romano, U. *J. Organomet. Chem.* **1978**, *154*, 323.
- (8) Gaffney, A. M.; Leonard, J. J.; Sofranko, J. A.; Sun, H. N. *J. Catal.* **1984**, *90*, 261.
- (9) Keller, N.; Rebmann, G.; Keller, V. *J. Mol. Catal. A: Chem.* **2010**, *317*, 1.
- (10) Miao, X. W.; Fischmeister, C.; Bruneau, C.; Dixneuf, P. H. *ChemSusChem* **2008**, *1*, 813.
- (11) Fabbri, D.; Bevoni, V.; Notari, M.; Rivetti, F. *Fuel* **2007**, *86*, 690.
- (12) *China Chemical Reporter*; 2010; <http://www.highbeam.com/doc/1G1-229228795.html>.
- (13) Pacheco, M. A.; Marshall, C. L. *Energy Fuels* **1997**, *11*, 2.
- (14) Xu, B.; Zhou, L.; Madix, R. J.; Friend, C. M. *Angew. Chem., Int. Ed.* **2009**, *49*, 394.
- (15) Xu, B.; Liu, X.; Haubrich, J.; Madix, R. J.; Friend, C. M. *Angew. Chem., Int. Ed.* **2009**, *48*, 4206.
- (16) Xu, B.; Liu, X.; Haubrich, J.; Friend, C. M. *Nat. Chem.* **2009**, *2*, 61.
- (17) Su, F. Z.; Liu, Y. M.; Wang, L. C.; Cao, Y.; He, H. Y.; Fan, K. N. *Angew. Chem., Int. Ed.* **2008**, *47*, 334.
- (18) Klitgaard, S. K.; DeLa Riva, A. T.; Helveg, S.; Werchmeister, R. M.; Christensen, C. H. *Catal. Lett.* **2008**, *126*, 213.
- (19) Lambert, R. M.; Williams, F. J.; Cropley, R. L.; Palermo, A. *J. Mol. Catal. A: Chem.* **2005**, *228*, 27.
- (20) Hayashi, T.; Tanaka, K.; Haruta, M. *J. Catal.* **1998**, *178*, 566.
- (21) Haruta, M.; Yamada, N.; Kobayashi, T.; Iijima, S. *J. Catal.* **1989**, *115*, 301.
- (22) Min, B. K.; Alemozafar, A. R.; Pinnaduwa, D.; Deng, X.; Friend, C. M. *J. Phys. Chem. B* **2006**, *110*, 19833.
- (23) Saliba, N.; Parker, D. H.; Koel, B. E. *Surf. Sci.* **1998**, *410*, 270.
- (24) Xu, B.; Madix, R. J.; Friend, C. M. *J. Am. Chem. Soc.* **2010**, *132*, 16571.
- (25) Xu, B.; Friend, C. M.; Madix, R. J. *Faraday Discuss.* **2011**, *152*, 241.
- (26) Wittstock, A.; Zielasek, V.; Biener, J.; Friend, C. M.; Baumer, M. *Science* **2010**, *327*, 319.
- (27) Gupte, S. P.; Shivarkar, A. B.; Chaudhari, R. V. *Chem. Commun.* **2001**, 2620.
- (28) Castonguay, M.; Roy, J. R.; Lavoie, S.; Adnot, A.; McBreen, P. H. *J. Am. Chem. Soc.* **2001**, *123*, 6429.
- (29) Worz, A. S.; Heiz, U.; Cinquini, F.; Pacchioni, G. *J. Phys. Chem. B* **2005**, *109*, 18418.
- (30) Carley, A. F.; Owens, A. W.; Rajumon, M. K.; Roberts, M. W.; Jackson, S. D. *Catal. Lett.* **1996**, *37*, 79.
- (31) Angelici, R. J. *J. Organomet. Chem.* **2008**, *693*, 847.
- (32) Nielsen, I.; Taarning, E.; Egeblad, K.; Madsen, R.; Christensen, C. *Catal. Lett.* **2007**, *116*, 35.
- (33) Andreasen, A.; Lynggaard, H.; Stegelmann, C.; Stoltze, P. *Surf. Sci.* **2003**, *544*, 5.
- (34) Wachs, I. E.; Madix, R. J. *Surf. Sci.* **1978**, *76*, 531.
- (35) Goguet, A.; Hardacre, C.; Harvey, I.; Narasimharao, K.; Saih, Y.; Sa, J. *J. Am. Chem. Soc.* **2009**, *131*, 6973.